

# ANODE MATERIAL FOR HIGH ENERGY DENSITY RECHARGEABLE LITHIUM-ION BATTERY

*Souichirou Suda, Yoshito Ishii and Tatsuya Nishida*  
*Inorganic Materials Division, Hitachi Chemical Co., Ltd., 3-3-1 Ayukawa, Hitachi, 316-0036 Japan*  
*Email: [s-suda@hitachi-chem.co.jp](mailto:s-suda@hitachi-chem.co.jp)*

## 1. Introduction

Fifteen years have passed since lithium-ion batteries were commercialized in 1991. Their energy density has increased by about 10% every year. Carbon anode material has greatly contributed to the increase through improving performance such as charge-discharge efficiency, discharge capacity, and applicable electrode density. Hitachi Chemical has commercialized high performance artificial anode material which possesses unique semispherical particle shape and highly graphitized crystal structure, and contains many pores which enable high speed Li-ion diffusion during charge-discharge<sup>(1)</sup>. At the moment, this kind of anode material is the best sold material. However, further improvement is required to meet higher energy density expectation of batteries to follow the advancement in mobile devices. In order to answer it, increase of anode electrode density was investigated. In this case, the performance will generally decrease due to several reasons. To approach the target, we have developed a new artificial graphite anode material by optimizing the micro- and macro-structures of graphite. This development has made possible the electrode density of higher than  $1.7 \times 10^3 \text{ kg/m}^3$ . Accordingly our development has contributed to the further advancement in battery performance. In this paper, we will report the electrode physical properties and electrochemical characteristics of the newly developed graphite.

## 2. Experimental

### 2-1. General properties of powder

Artificial graphite powders AGP-A(conventional) and AGP-B(developed) were investigated as anode materials. General properties such as average particle size, N<sub>2</sub>-BET specific surface area, pore volume measured with a porosimeter, tapping density, ash content, and true density were shown in Table 1.

### 2-2. Preparation of electrode

SBR binder (BM-400B from Nippon Zeon) and CMC as the viscosity preparation agent (#2200 from Daicel Corp.) were used. The contents of graphite/SBR/CMC were 98/1/1 by weight. After dispersed in water, it was coated on a copper foil, was pressed by controlling thickness and density, and then was dried in an oven.

### 2-3. Orientation of electrode

The orientation of the electrode was defined as the strength ratio of (002)/(110) peak in the X-ray diffraction analysis.

### 2-4. Absorption speed of electrolyte solvent

The absorption speed was evaluated as the time for complete absorption after 1 $\mu$ L of electrolyte solvent was dropped onto the electrode. 1M LiPF<sub>6</sub> EC+EMC (3:7) was used as the solvent.

### 2-5. Charge-discharge properties

The charge-discharge properties were evaluated using a coin type cell. Li metal was used as the counter, and 1M LiPF<sub>6</sub> EC+EMC (3:7) as the electrolyte. The charging current density was 2.8 A/m<sup>2</sup> till 0 V, and 0.28 A/m<sup>2</sup> cut in constant voltage. The discharge current density was 2.8 A/m<sup>2</sup> and 1.5 V cut.

## 3. Results and discussion

### 3-1. Powder properties of materials

Figure 1 shows the sectional SEM images of graphite particles. Both AGP-A and AGP-B have a similar peculiar semispherical shape. As shown in Table 1, AGP-B has smaller pore volume, larger tapping density, and lower BET surface compared with AGP-A. We thought that the difference in microstructure will be related to the difference of powder properties.

### 3-2. Orientation of electrode

Figure 2 shows the change of orientation with electrode density measured by the X-ray diffraction. In general, (002) diffraction is originated from the extent of layer direction, and (110) diffraction from the perpendicular direction. In general, the crystal structure of graphite (002) is much bigger than that of (110), and the ratio of intensity (002)/(110) is specified as the orientation. When the anode material shows lower orientation, that is, larger (110) extent is better to get smooth diffusion of Li-ion during charge-discharge. However, increase of electrode density which adds the loading pressure in the perpendicular direction will lead to further orientation.

In this investigation the increase of orientation with electrode density was lower for AGP-B than for AGP-A. We considered that fewer pores should prevent the deformation of particles by loading. AGP-A which contains more pores is quite soft and it will deform by loading with the increase in density. The deformation of particles will give rise to the further orientation of crystal structures, which is less of (110), and more of (002).

### 3-3. Absorption property of electrolyte

Figure 3 shows the absorption speed of electrolyte for different electrode densities. It indicated that the index value of 100 for AGP-A is  $1.60 \times 10^3 \text{ kg/m}^3$ . In this investigation AGP-B was able to absorb in shorter time than AGP-A at 1.60 and  $1.73 \times 10^3 \text{ kg/m}^3$  respectively. The main reason will be that AGP-B has larger gaps between particles which will play the role of passages for electrolyte absorption. This difference will also be resulted from the difference of particle structure.

Charge and discharge will run consuming the electrolyte solvent. Less absorption will lead to faster dry-up of electrolyte and to discharge capacity decrease during cycling. In addition, absorption property is important not only for performance but also for productivity of the battery. AGP-B has superiority over AGP-A in both performance and process cost.

### 3-4. Charge-discharge properties

Table 2 shows the first cycle charge-discharge properties. AGP-B showed a discharge capacity of 360 Ah/kg, the same level as AGP-A. It means that the difference in particle structure has no influence on discharge capacity. However, regarding the irreversible loss at 1st cycle, AGP-B was lower than AGP-A, which is better for the battery capacity requiring less consumption of irreversible cathode. We considered that the loss at 1st cycle is caused by the decomposition of electrolyte and that this is strongly related to the BET surface. In this viewpoint, the BET surface of AGP-B is lower than that of AGP-A as shown in Table 1.

Figure 4 shows the 1st cycle charge-discharge curves for AGP-A and AGP-B. The curves showed a plateau caused by the structural change of Li-graphite intercalation compound that is typical for crystallized graphite. There is no difference between AGP-A and AGP-B in this character.

Figure 5 shows the relationship between the charge-discharge efficiency at 1st cycle and the electrode density. The efficiency generally decreases as the electrode density increases. In the whole range of density, AGP-B kept higher efficiency than AGP-A. Figure 6 shows the relationship between the discharge capacity and the discharge current density. These properties are extremely important factors indicating the capability in harsh circumstances consuming large current. Discharge capacity will normally decrease as current density increases. It indicates that the polarization resistance of the electrode increases. In this investigation AGP-B shows higher discharge capacity retention in any current density. These properties are caused by the difference in the easiness of Li-ion diffusion. As described above, AGP-B has lower orientation of crystal structure especially at high electrode density. We considered that the lower orientation will enable smooth diffusion of Li-ion during charge-discharge. Pore volume will certainly contribute to the performance of the anode. However, the role of pore varies with the increase in electrode density. Large volume of pore will make the deformation of particles possible and promote the orientation of crystal structure under high electrode density which adds high loading pressure in layer direction. In order to get best performance, the optimization of pore volume is inevitable.

## 4. Conclusions

- (1) The relationship was investigated between orientation of crystal structure that is an important factor controlling the performance of anode material and the particle properties including pore structure. As a result, it was clarified that the orientation will be restrained by decreasing the pore volume in the high electrode density region.
- (2) The newly developed anode material AGP-B having lower pore volume and lower BET surface showed lower irreversible capacity and higher discharge capacity retention at larger current density.
- (3) The development of new graphite having better performance with high electrode density will make possible the design of Li-ion batteries with higher energy density.

## 5. References

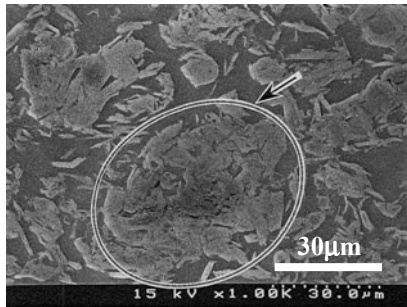
- (1) Y. Ishii *et al.*: Hitachi Chemical Technical Report, No. 36, p. 27(2001).

**Table 1.** Powder properties

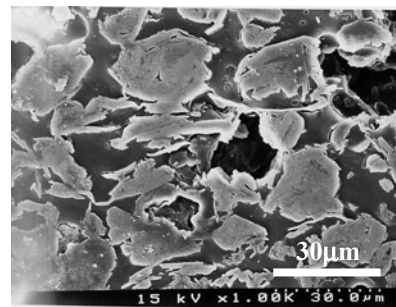
Items	AGP-A	AGP-B
Average particle size( $\mu\text{m}$ )	20	24
$\text{N}_2$ -BET specific surface area( $\times 10^3 \text{ m}^2/\text{kg}$ )	4.0	3.3
Pore volume( $\times 10^{-3} \text{ m}^3/\text{kg}$ )	0.9	0.7
30 times tapping density( $\times 10^3 \text{ kg/m}^3$ )	0.65	0.73
Ash content(%)	0.02	0.02
True specific gravity(-)	2.24	2.24

**Table 2.** First cycle charge-discharge properties

Items	AGP-A	AGP-B
Charge capacity(Ah/kg)	384	379
Discharge capacity(Ah/kg)	362	360
Irreversible capacity(Ah/kg)	22	19
Charge-discharge efficiency (%)	94.3	95.0



(a) AGP-A



(b) AGP-B

**Figure 1.** Sectional SEM images of graphite particles

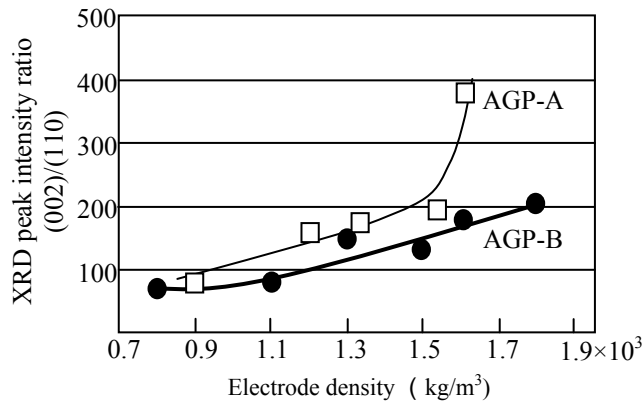


**Figure 2.** Relationship between electrode density and XRD peak intensity ratio(002)/(110)

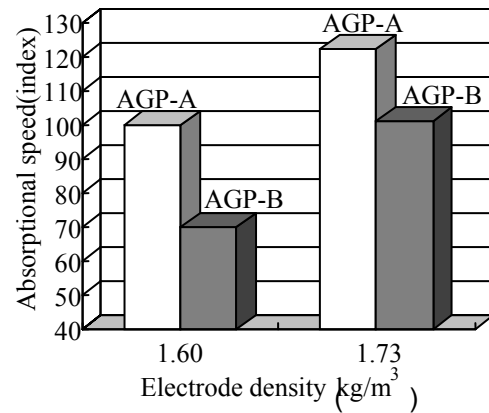


**Figure 3.** Time index for electrolyte absorption

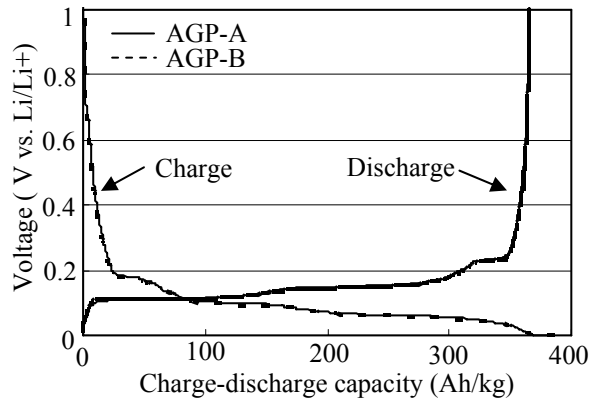


**Figure 4.** First cycle charge-discharge curves for AGP-A and AGP-B

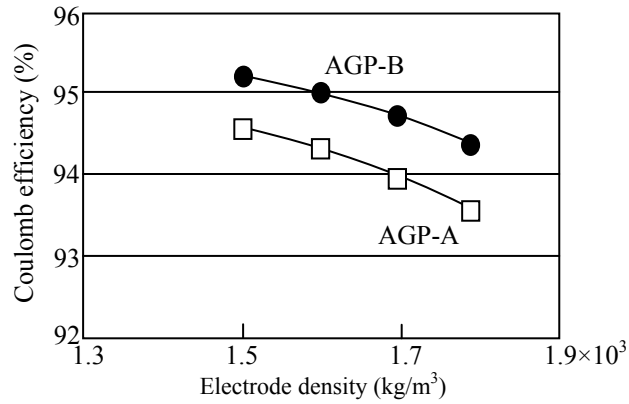


**Figure 5.** Relationship between electrode density and first charge-discharge efficiency

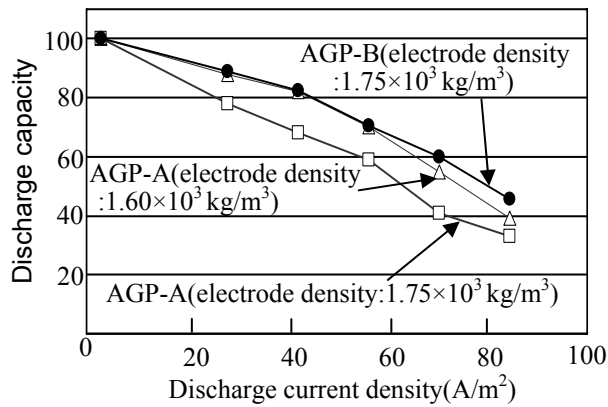


**Figure 6.** Relationship between discharge current density and discharge capacity retention